



Auxin Distribution in Lateral Root Primordium Development Affects the Size and Lateral Root Diameter of Rice

Tsubasa Kawai^{1,2}, Ryosuke Akahoshi¹, Israt J. Shelley^{3,4}, Takaaki Kojima¹, Moeko Sato⁵, Hiroyuki Tsuji⁵ and Yoshiaki Inukai^{3*}

¹ Graduate School of Bioagricultural Sciences, Nagoya University, Nagoya, Japan, ² School of Agriculture and Environment, The UWA Institute of Agriculture, The University of Western Australia, Perth, WA, Australia, ³ International Center for Research and Education in Agriculture, Nagoya University, Nagoya, Japan, ⁴ Department of Crop Botany, Bangladesh Agricultural University, Mymensingh, Bangladesh, ⁵ Kihara Institute for Biological Research, Yokohama City University, Yokohama, Japan

OPEN ACCESS

Edited by:

Ran Xu,
Hainan University, China

Reviewed by:

Mukesh Jain,
Jawaharlal Nehru University, India
Doan Trung Luu,
Centre National de la Recherche
Scientifique (CNRS), France

*Correspondence:

Yoshiaki Inukai
inukaiy@agr.nagoya-u.ac.jp

Specialty section:

This article was submitted to
Plant Development and EvoDevo,
a section of the journal
Frontiers in Plant Science

Received: 13 December 2021

Accepted: 07 March 2022

Published: 13 April 2022

Citation:

Kawai T, Akahoshi R, Shelley IJ, Kojima T, Sato M, Tsuji H and Inukai Y (2022) Auxin Distribution in Lateral Root Primordium Development Affects the Size and Lateral Root Diameter of Rice. *Front. Plant Sci.* 13:834378. doi: 10.3389/fpls.2022.834378

Lateral roots (LRs) occupy a large part of the root system and play a central role in plant water and nutrient uptake. Monocot plants, such as rice, produce two types of LRs: the S-type (short and thin) and the L-type (long, thick, and capable of further branching). Because of the ability to produce higher-order branches, the L-type LR formation contributes to efficient root system expansion. Auxin plays a major role in regulating the root system development, but its involvement in developing different types of LRs is largely unknown. Here, we show that auxin distribution is involved in regulating LR diameter. *Dynammin-related protein (DRP)* genes were isolated as causative genes of the mutants with increased L-type LR number and diameter than wild-type (WT). In the *drp* mutants, reduced endocytic activity was detected in rice protoplast and LRs with a decreased OsPIN1b-GFP endocytosis in the protoplast. Analysis of auxin distribution using auxin-responsive promoter *DR5* revealed the upregulated auxin signaling in L-type LR primordia (LRP) of the WT and the mutants. The application of polar auxin transport inhibitors enhanced the effect of exogenous auxin to increase LR diameter with upregulated auxin signaling in the basal part of LRP. Inducible repression of auxin signaling in the mOs/AA3-GR system suppressed the increase in LR diameter after root tip excision, suggesting a positive role of auxin signaling in LR diameter increase. A positive regulator of LR diameter, *OsWOX10*, was auxin-inducible and upregulated in the *drp* mutants more than the WT, and revealed as a potential target of ARF transcriptional activator. Therefore, auxin signaling upregulation in LRP, especially at the basal part, induces *OsWOX10* expression, increasing LR diameter.

Keywords: lateral root, root development, dynammin-related protein, auxin distribution, rice

INTRODUCTION

The root system in rice comprises main roots, including an embryonic seminal root (SR) and shoot-borne crown roots (CRs), and their lateral roots (LRs). LRs are classified as S- and L-types based on their distinct morphological and anatomical characteristics (Kawata and Shibayama, 1965; Kono et al., 1972; Yamauchi et al., 1987). S-type LRs are thinner and shorter than L-types, and never produce higher order LRs. S-type LRs largely contribute to the hydraulic conductivity of the whole root system (representing water uptake ability) (Watanabe et al., 2020), while L-type LRs expand the root network in soils by producing higher-order LRs including both S- and L-types. The plastic development of LRs plays an important role for the adaptation to soil water fluctuation of rice (Suralta et al., 2018; Lucob-Agustin et al., 2021).

Plant hormone auxin plays a central role in LR formation. Under low auxin levels, Aux/IAA proteins repress auxin-responsive transcription (Ramos et al., 2001). Auxin perception by its receptor TIR1/AFB (Tan et al., 2007) promotes the ubiquitination of Aux/IAA by the TIR1/AFBs complex (Gray et al., 2001). The degradation of the ubiquitinated Aux/IAA by 26S proteasome allows auxin-responsive transcriptional regulation by ARF proteins (Gray et al., 2001). The core sequence GWPPV in domain II of Aux/IAA is required for the auxin-responsive ubiquitination of Aux/IAA, and mutations in the core sequence inhibit the auxin signaling transmission (Ramos et al., 2001). The gain-of-function mutants of Aux/IAA, from a stabilizing mutation in their domain II, decreased the number of LRs in *Arabidopsis* (e.g., Fukaki et al., 2002) and rice (e.g., Kitomi et al., 2012).

Auxin distribution regulated by its polar transport is crucial for root system development. The differential distribution of auxin is produced mainly by the AUXIN1/LIKE-AUX1 (AUX1/LAX) influx carrier and PIN-FORMED (PIN) efflux carriers in rice roots (Yu et al., 2016). The mutation in *OsAUX1* causes defects in LR formation and root hair elongation (Zhao et al., 2015). Additionally, the over-expression of *OsPIN1b* increases LR density (Xu et al., 2005) and the *Ospin1a Ospin1b* double mutant decreases lateral and crown root numbers (Li et al., 2019). In *Ospin2* mutant, the basipetal shifting of LR formation pattern was observed with higher auxin content in the SR tip (Inahashi et al., 2018). In *Arabidopsis*, auxin distribution changes dynamically during LR formation—auxin accumulates in pericycle cells that differentiate into LR primordia (LRP); then, gradual auxin distribution is established and maximized at the root tip by PIN proteins (Benková et al., 2003). A synthetic compound, *N*-1-naphthylphthalamic acid (NPA), has been used to study the role of polar auxin transport in plant tissue development, which directly binds to PIN auxin transporters and inhibits its IAA transport activity (Abas et al., 2021). In rice,

NPA treatment inhibited LR formation with restricted lateral flow of auxin from the main roots to the LRs (Sreevidya et al., 2010). Therefore, proper auxin distribution by PIN proteins is important for LR formation.

Regulatory mechanisms of cellular localization of the PIN protein, crucial for directing auxin flow, have been well studied in *Arabidopsis* (Luschnig and Vert, 2014). During LR formation in *Arabidopsis*, PIN1 cellular localization changes from anticlinal to periclinal sides, which is crucial for establishing the auxin gradient and, thus, proper LR formation (Benková et al., 2003). Polar localization of PIN proteins is established by targeted exocytosis and endocytosis pathways. Guanine nucleotide exchange factors for ADP ribosylation factors (ARF-GEFs) mediate PIN exocytosis to the rootward plasma membrane in *Arabidopsis* roots, which is sensitive to a fungal toxin brefeldin A (BFA) (Steinmann et al., 1999; Geldner et al., 2003). BFA treatment inhibited the re-direction of PIN1 protein during LR formation in *Arabidopsis* (Benková et al., 2003). In rice, the mutation in ARF-GEF *CRL4/OsGNOM1* caused defects in crown and lateral root formation (Kitomi et al., 2008; Liu et al., 2009). Clathrin-mediated endocytosis (CME) has a central role in PIN protein endocytosis (Dhonukshe et al., 2007; Kleine-Vehn et al., 2011; Kitakura et al., 2011). Dynamin is a large GTPase and functions in membrane scission of the clathrin-coated vesicles. In plants, dynamin-related proteins DRP1 and DRP2 are involved in CME (Fujimoto et al., 2010). In *Arabidopsis*, loss-of-function of *DRP1A* caused defects in auxin-related developmental phenotypes (Mravec et al., 2011). Regulatory mechanisms of auxin distribution and its function for root formation have been well-studied; however, the involvement of auxin distribution in the LR type determination in rice is poorly understood.

Lateral roots are derived from the pericycle and endodermal cells of the main roots in rice. The LR type is characterized during the LRP stage with distinct size of meristem formed in the two types (Kawata and Shibayama, 1965; Kawai et al., 2022a). Root tip excision was used to analyze the molecular mechanisms underlying the control of LRP size, which promotes L-type LR formation (Sasaki et al., 1984; Kawai et al., 2017, 2022b). Transcriptome analysis suggested the upregulation of auxin signaling in L-type LRP than S-types, which possibly induces the expression of *OsWOX10*, a positive regulator of LR diameter (Kawai et al., 2022a). In another study, a rice mutant, *weg1*, was selected for its promoted L-type LR formation with a wavy main root phenotype (Lucob-Agustin et al., 2020). Observation of auxin signaling using a fluorescent protein driven by the auxin-responsive promoter *DR5* revealed the upregulation of auxin signaling on the convex side of curvature where L-type LRs develop (Lucob-Agustin et al., 2020). The secondary LR development is positively regulated by auxin and inhibited by strigolactone signaling (Sun et al., 2019). These studies suggest the involvement of auxin in determining the LR type. However, how the two types of LRP differ in spatiotemporal auxin distribution remains unclear.

In this study, we isolated novel rice mutants with thicker LRs than wild-type (WT). Map-based cloning revealed *DRP* family genes as the causative genes of mutants. The auxin signaling

Abbreviations: AuxRE, Auxin response element; BFA, Brefeldin A; CME, Clathrin-mediated endocytosis; CR, Crown root; DEX, Dexamethasone; DRP, Dynamin-related protein; EMSA, Electrophoresis mobility shift assay; GR, Glucocorticoid receptor; IAA, Indole-3-acetic acid; LR, Lateral root; LRP, Lateral root primordial; MNU, *N*-methyl-*N*-nitrosourea; NPA, *N*-1-naphthylphthalamic acid; SD, Standard deviation; SR, Seminal root; WT, Wild-type.

distribution in LRP revealed different distribution patterns in the WT and the mutants. Exogenous treatment of auxin and its polar transport inhibitors further suggested the regulation of LR diameter through auxin distribution in LRP.

MATERIALS AND METHODS

Plant Material and Growth Conditions

N-methyl-*N*-nitrosourea (MNU) mutagenized population of rice plants (*Oryza sativa* L. cv. “Taichung 65”) was obtained using the panicle-dipping method (Sato and Omura, 1979). Treated panicles were harvested to obtain M₁ seeds, which were grown to obtain M₂ seeds. Rice seedlings were grown hydroponically. Rice seeds were pregerminated in water mixed with fungicide [0.25% (w/v) benomyl benlate; Sumitomo Chemical Co., Japan] and placed in a growth chamber (MLR-351; Sanyo, Japan) at 28°C with continuous light for 3 days. Germinated seeds were rinsed with tap water and transferred onto plastic nets floating on 10% nutrient solution (Colmer, 2003) aerated with a pump (OX-30; Tetra-Japan, Japan) in a 9-L black plastic box (32 cm height × 19 cm length × 19 cm width). For map-based cloning, seeds of the WT, mutants, and F₂ plants derived from crosses between the mutants and *O. sativa* “Kasalath” were grown for 2 weeks. For inducing L-type LR formation in *DR5-NLS-3xVENUS* and *pOsAct1-mOsIAA3-GR*, CRs of approximately 10 cm length were excised at 5 mm from the root tip with a cutting knife. To analyze the LR formation in *pOsAct1-mOsIAA3-GR*, transgenic plants were transferred prior to the root tip excision to the solution containing 50 μM dexamethasone (DEX) for different durations. The transgenic plants after the root tip excision were grown under the DEX condition for another 3 days. For chemical treatments, 4-day-old WT and mutants’ seedlings were transferred to tap water filtered by a water purifier (MX600; TORAY Industries, Japan) containing IAA and/or inhibitor (1 μM NPA or BFA) and grown for another 10 days.

Morphological Characterization

To characterize LR phenotypes in the WT and mutants, the SRs of 10-day-old seedlings were sampled and fixed in FAA solution [5 formaldehyde, 5 acetic acid, 63% ethanol (v/v)]. The LR number on sampled SRs in three diameter classes (<100 μm, S-type; ≥ 150 μm, L-type; 100–150 μm, intermediate type) was counted. The density of LRs was calculated as the LR number divided by the length of SR formed LRs. The diameter and length were measured in LRs emerged on the basal part of SRs (2–4 cm). The root segments were fully extended on a slide and images were taken with a digital camera (D90; Nikon, Japan). Diameters of the first-order LRs were measured in the basal region using a microscope (IX71; Olympus, Japan) and a micrometer. Lengths of the first-order LRs were measured from images using LIA for Win32.¹

To characterize LR phenotypes in the WT and mutants with chemical treatments, SR length and the length of LR-formed region were recorded when the seedlings were transferred to

the treatment solution. SR segments corresponding to the region without LRs at transfer were sampled for LR measurement.

Map-Based Cloning, Plasmid Constructs, and Plant Transformation

The linkage analysis of SSR (simple-sequence repeats) markers was performed using the F₂ plants derived from crosses between each mutant and “Kasalath.” For T12-3, T3-2, and T12-36, 779, 13, and 443 F₂ plants that exhibited the mutant phenotype were used for the linkage analysis, respectively. To complement the mutation, *pOsDRP1C-OsDRP1C-GFP* construct was transformed into T12-3. The genomic sequence of *OsDRP1C* from approximately –3 kb to –1 bp (*OsDRP1C* translation start site: + 1 bp) and the coding sequence of *OsDRP1C* were amplified from “Taichung 65” genomic and complementary DNA, respectively, and cloned into pENTR/D-TOPO®. The *pOsDRP1C-OsDRP1C* fragment was then transferred into the pGWB4 vector (Nakagawa et al., 2007) using the Gateway LR reaction. For the transient expression of *OsPIN1b-GFP* in rice protoplast, *p35S-OsPIN1b-GFP* was transformed into protoplasts of the WT and mutants. The coding sequence of *OsPIN1b* was amplified from “Taichung 65” complementary DNA, fused to *GFP* derived from the pGWB4 vector, then cloned into pGWB502Ω vector harboring 2 × 35S promoter with translation enhancer (Nakagawa et al., 2007). The *35S-OsPIN1b-GFP* fragment with NOS terminator was then transferred into pENTR/D-TOPO®. The *DR5-NLS-3xVENUS* was constructed as previously described (Lucob-Agustin et al., 2020). The *pOsAct1-mOsIAA3-GR* was constructed as previously described (Nakamura et al., 2006). Briefly, the coding sequence of *OsIAA3* (Os12g0601400) was amplified and a nucleotide substitution in domain II (P58L) by PCR was introduced and then fused to the *pAct-GR-Hm2* vector harboring rice *Actin 1* promoter and the steroid-binding domain of the human GR. The primers used in this study are listed in **Supplementary Table 1**. The fusion constructs were introduced into *Agrobacterium tumefaciens* strain EHA105 by electroporation. The *Agrobacterium*-mediated transformation of rice was then performed as described elsewhere (Hiei et al., 1994; Ozawa, 2009). Transgenic plants were selected on Murashige and Skoog (MS) medium containing 50 mg/l hygromycin at 30°C.

Microscopic Observation

Crown root sections were sampled to observe *DR5-NLS-3xVenus* expression in the LRP of the WT and mutants. The samples were fixed in 4% paraformaldehyde (w/v) and stained with 5 μg/ml DAPI (4',6-Diamidino-2-phenylindole Dihydrochloride; Wako, Japan) for 1 h, then cleared with iTOMEI (TCI, Japan) (Sato et al., 2022; Sakamoto et al., 2022), or embedded in a 3% (w/v) agar medium then cross-sectioned into 50 μm thick slices with a linear slicer (DYK-1000N; Dosaka EM Co., Japan). The samples were viewed under a confocal laser scanning microscope (FV3000; Olympus, Japan). Venus fluorescence was excited at 488 nm and detected at 510–530 nm, while DAPI or autofluorescence of the root samples was excited at 405 nm and detected at 450–470 nm.

¹<https://www.agr.nagoya-u.ac.jp/~shinkan/LIA32>

We have confirmed that the WT and mutants' phenotypes were not affected by the transformation.

Expression Analysis

Total RNA was extracted from SR segments including the earlier stage of LRP (Part 3 in **Supplementary Figure 4A**) in 5-day-old seedlings using the NucleoSpin[®] RNA Plant Kit (Macherey-Nagel, Germany) following the manufacturer's instructions. Quantitative reverse-transcription PCR (qRT-PCR) was performed using the One-Step SYBR PrimeScript RT-PCR Kit II (Perfect Real-Time) (TaKaRa Bio, Japan) and StepOnePlus Real-Time PCR (Life Technologies, United States). The expression was normalized to that of *OsUBQ5* (Os03g0234200). All primers are listed in **Supplementary Table 1**. The expression of *OsDRP* family genes was compared using the RNA-seq data in S- and L-type LRP with four biological replications (Kawai et al., 2022a). The read counts were normalized by coding sequence length (per 1 kb) for all genes in each replicate to calculate transcript per million (TPM). The normalized read counts were further normalized by summing the normalized counts of all genes (per million reads). Means of the calculated TPMs of four biological replications were used to compare the expression levels between S- and L-type LRP. The significance of the difference between S- and L-type LRP was determined by *Padj* values calculated by DESeq2 (Love et al., 2014).

Transient Expression in Rice Protoplast

For the protoplast isolation, rice seedlings of the WT and mutants were grown in 1/2 MS medium. For the first 3 days, rice seeds were placed on the medium in the growth chamber at 28°C with continuous light to promote seed germination, then transferred to the dark condition to reduce the autofluorescence from chloroplast. Protoplasts were isolated from the stem and sheath of 2-week-old seedlings as previously described (Zhang et al., 2011). Briefly, 20 µg of the plasmid DNA was mixed with 100 µl protoplasts (2×10^5 cells), then transformed *via* PEG. The transformed protoplasts with *OsPIN1b-GFP* were treated with 10 µM FM4-64 (Setareh Biotech, United States) for 30 min at room temperature, then viewed under the confocal laser scanning microscope. GFP fluorescence was excited at 488 nm and detected at 500–540 nm, while FM4-64 was excited at 561 nm and detected at 570–620 nm.

FM4-64 Uptake Assay in Rice Roots

To test the endocytic activity, WT and mutants' seedlings were grown in the 10% nutrient solution for 6 days, then transferred to the solution containing 10 µM FM4-64. After 30 min treatment of FM4-64 at room temperature, S-type LRs were sampled and immediately viewed under the confocal laser scanning microscope as described above.

Electrophoresis Mobility Shift Assay

The binding of OsARF19, preferentially expressed in LRP (Yamauchi et al., 2019), to auxin response elements (AuxREs) on *OsWOX10* promoter was analyzed by performing an electrophoresis mobility shift assay (EMSA). The sequence encoding the N-terminal 265 amino acids of OsARF19, including the B3 DNA-binding domain (DB), that was optimized for the

codon usage of *E. coli*, was fused to pET32a. The OsARF19-DB was expressed in *E. coli* BL21(DE3), followed by purification with TALON metal affinity resin (Clontech, United States) following the manufacturer's instructions. To prepare DNA probes, the 59 or 60-bp oligonucleotides were labeled with Cy5 fluorescence dye using Klenow fragment (TaKaRa Bio, Japan) and purified on a column (NucleoSpin[®] Gel and PCR Clean-up; Macherey-Nagel, Germany) following the manufacturer's instructions. The DNA-binding reaction was performed at 4°C for 30 min in PBS (-) (137 mM NaCl, 8.10 mM Na₂HPO₄, 2.68 mM KCl, 1.47 mM KH₂PO₄; pH 7.4) + 1 mM 2-Mercaptoethanol with 25.3 nM probe with 0, 0.5, or 1 µM recombinant OsARF19-DB, and subjected to EMSA with 5% polyacrylamide gels in 0.5 × TBE buffer at 4°C. The Cy5-labeled probes were analyzed by Typhoon FLA9000 (GE Healthcare, United States).

Statistical Analysis

Differences in morphological and anatomical characteristics, and gene expression between groups were compared using two-tailed Student's *t*-test or one-way ANOVA and a multiple-comparison Tukey's test using the *glht* function from *multcomp* package in R (R Core Team, 2020).

RESULTS AND DISCUSSION

Identification of Mutants With Promoted L-Type Lateral Root Formation

MNU-mutagenized populations were analyzed for their root formation to study the molecular mechanisms underlying the control of LRP size. The three mutants had fewer thinner LRs (< 150 µm in diameter) and thicker LRs (≥150 µm in diameter) than the WT (**Figures 1A–D**). Total LR number decreased in the three mutants (**Supplementary Figure 1A**). The number of LRs forming second-order LRs increased in T3-2 and T12-36 compared to the WT (**Figure 1E**). Furthermore, the LR diameter of the thickest LRs increased in the three mutants (**Figure 1F**). The lengths of the thinner LRs decreased in T3-2 and T12-3, and the length of the thicker LRs also decreased in T12-3, compared to the WT (**Supplementary Figures 1B,C**). The mutants also had a shorter SR than the WT, with the shortest SR in T12-3 (**Supplementary Figure 1D**). In T12-3, the CR number slightly increased than the WT (**Supplementary Figure 1E**). The mutants had shorter leaf lengths than the WT (**Supplementary Figure 1F**).

Isolation of the Mutants' Causative Genes

Linkage analyses of SSR markers were undertaken using the F₂ plants derived from crosses between each mutant and "Kasalath" to identify the causative genes of mutants. The root phenotype of the mapping populations was segregated in a 3:1 WT:mutant ratio in the linkage analyses. In T12-36, the linkage analysis revealed the locus on chromosome 2 between RM5472 and RM13949 (~324 kb) (**Figure 2A**). This region contains around 50 genes including *OsDRP2B* (*Dynamamin-related protein 2B*, Os02g0738900). Comparison of the sequences between the WT

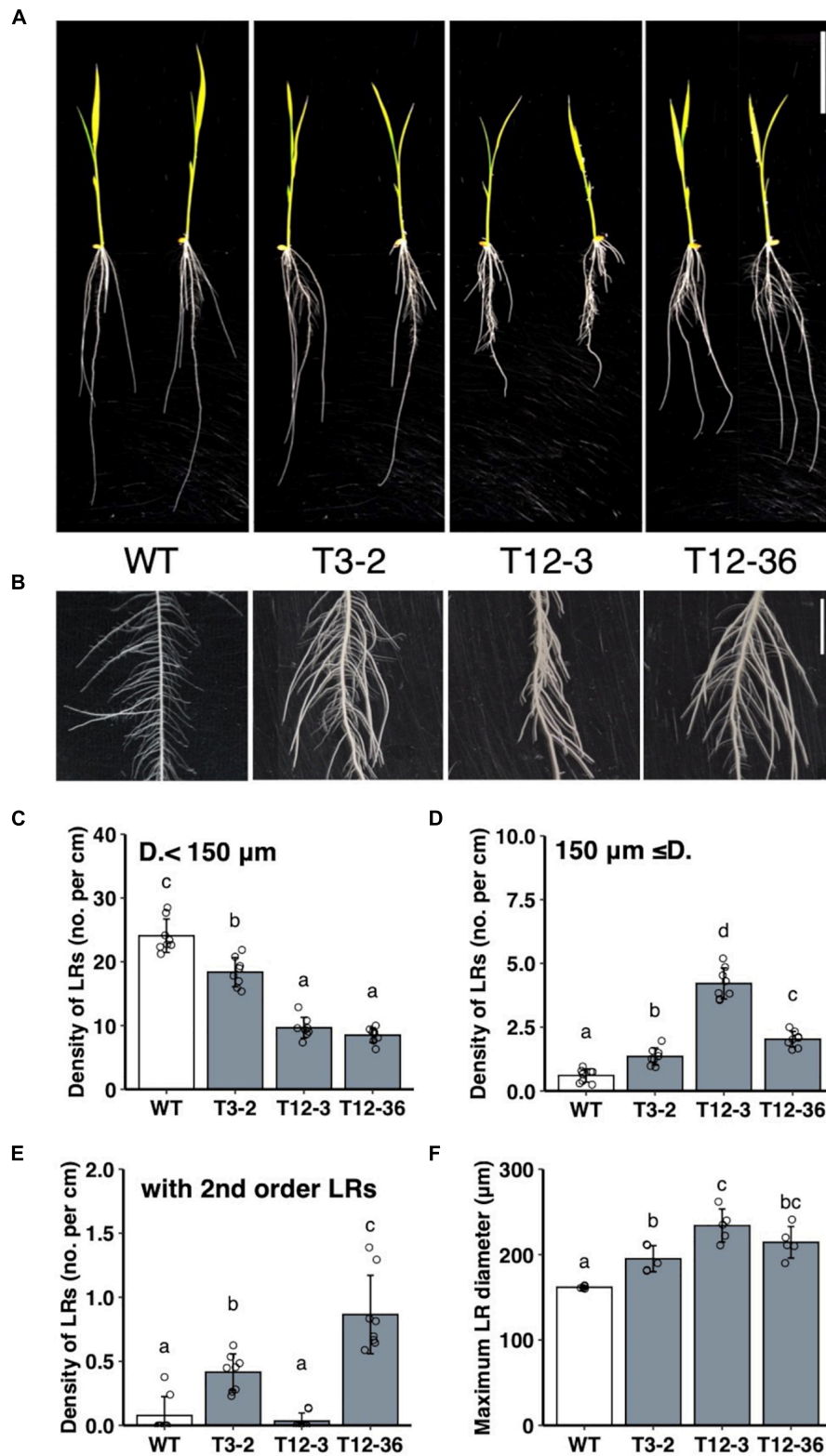
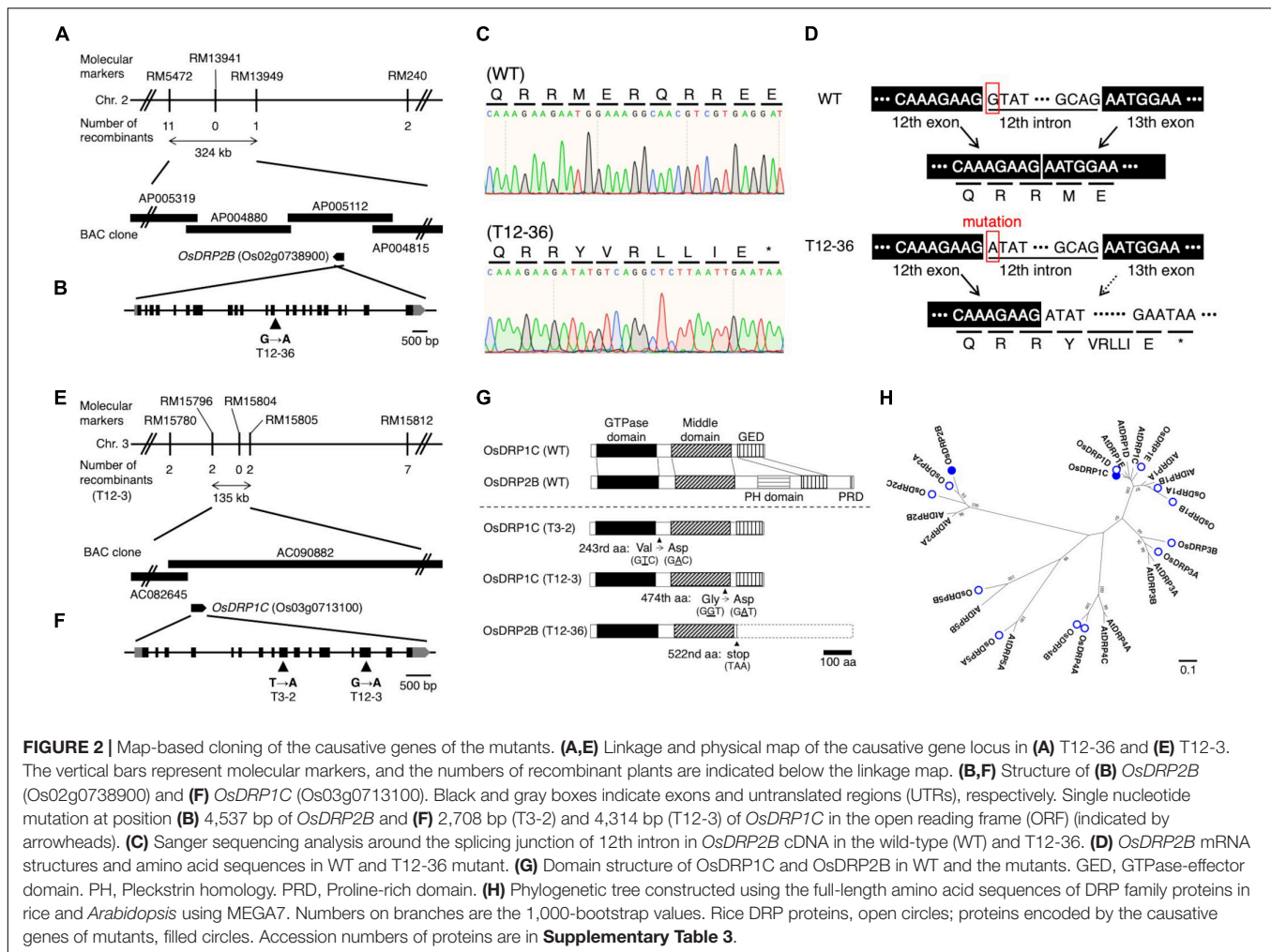


FIGURE 1 | Analysis of lateral root (LR) formation on seminal roots (SRs) in 10-day-old seedlings of the wild-type (WT) rice and mutants (T3-2, T12-3, and T12-36). **(A)** Shoot and root phenotypes. Two representative plantlets are shown. Scale bar = 5 cm. **(B)** LR phenotypes on SRs. Scale bar = 1 cm. **(C,D)** Density of LRs in two different diameter classes. D., LR diameter. **(E)** Density of first-order LRs forming second-order LRs. **(F)** Maximum LR diameter. Values represent mean \pm SD [$n = 8$ **(C–E)** and 5 **(F)** independent biological replicates]. Different letters indicate significant differences among genotypes ($P < 0.05$).



and T12-36 revealed a single nucleotide substitution from G to A in the 12th intron (**Figure 2B**). As the mutated site was likely important for splicing in *OsDRP2B*, we compared the mRNA sequence by synthesizing cDNA from the WT and mutant. The splicing of the 12th intron was defective in T12-36, causing a stop codon after the 12th exon (**Figures 2C,D**). DRP2 proteins have five functional domains like the animal dynamin, while DRP1 proteins lack a PH (Pleckstrin homology) domain and a PRD (Proline-rich domain), which function in association with the cell membrane and actin (Schmid and Frolov, 2011; **Figure 2G**). T12-36 might produce a truncated *OsDRP2B* protein without a PH domain, GED (GTPase-effector domain), and PRD (**Figure 2G**). In previous studies, *OsDRP2B* was isolated as the causative gene of *brittle culm 3* (*bc3*) mutant (Hirano et al., 2010; Xiong et al., 2010), as observed in T12-36 in the present study (**Figure 1** and **Supplementary Figure 1**), indicating that T12-36 is an allelic mutant of the previously reported *bc3* mutant.

In T12-3, the linkage analysis revealed the locus on chromosome 3 between RM15796 and RM15805 (~135 kb) (**Figure 2E**). This region contains 14 genes including *OsDRP1C*

(*Dynamamin-related protein 1C*, Os03g0713100). Comparing the WT and mutant sequences revealed a single nucleotide substitution, from G to A in the 14th exon (**Figure 2F**). In T3-2, a rough mapping revealed the locus between RM15414 and RM3199 (~8 Mb), which contains the mapped region in T12-3. Therefore, we compared the *OsDRP1C* sequence between the WT and T3-2, detecting a single nucleotide substitution from T to A in the 9th exon (**Figure 2F**). In T12-3, the nucleotide substitution causes Gly to Asp amino acid substitution in the middle domain, mediating the protein interaction between dynamins (Ramachandran et al., 2007), while the mutation in T3-2 causes Val to Asp amino acid substitution between GTPase and middle domain of *OsDRP1C* (**Figure 2G**). The more distinct phenotypes in T12-3 than T3-2 (**Figure 1** and **Supplementary Figure 1**) are possibly associated with the mutation sites in these two mutants. The introduction of ~3 kb promoter and the coding sequence of *OsDRP1C* into T12-3 complemented the mutant phenotype (**Supplementary Figure 2**), confirming that *OsDRP1C* is the causative gene of T12-3.

In rice, there are 14 dynamin family proteins, classified into six groups (**Figure 2H**). The DRP1 and DRP2 proteins function in post-Golgi trafficking in *Arabidopsis* (Fujimoto et al., 2010).

OsDRP2B localized in the plasma membrane, clathrin-mediated vesicles, and *trans*-Golgi network, involving in the endocytic pathway (Xiong et al., 2010). Co-expression of *OsDRP1C* and *OsDRP2B* was detected in a rice co-expression network database (RiceFRIEND; Sato et al., 2013a; **Supplementary Table 2**). In a public rice gene expression database (RiceXPro; Sato et al., 2013b), *OsDRP1C* and *OsDRP2B* had similar expression patterns among plant organs and tissues with relatively higher expression in leaf sheath and stems, roots, and reproductive tissues (**Supplementary Figure 3**). The *OsDRP1C* and *OsDRP2B* genes along the SR axis had similar expressions, with relatively higher expressions in the LR emerged region (**Supplementary Figures 4A–C**). Based on the RNA-seq result in S- and L-type LRP in the WT (Kawai et al., 2022a), *OsDRP1C* and *OsDRP2B* were highly expressed in S- and L-type LRP, relative to other *OsDRP* genes (**Supplementary Figure 4D**). Thus, these two rice DRPs may cooperate in CME, involving in LR diameter control.

Altered PIN Protein Localization With Reduced Endocytic Activity in *Dynamin-Related Protein* Mutants

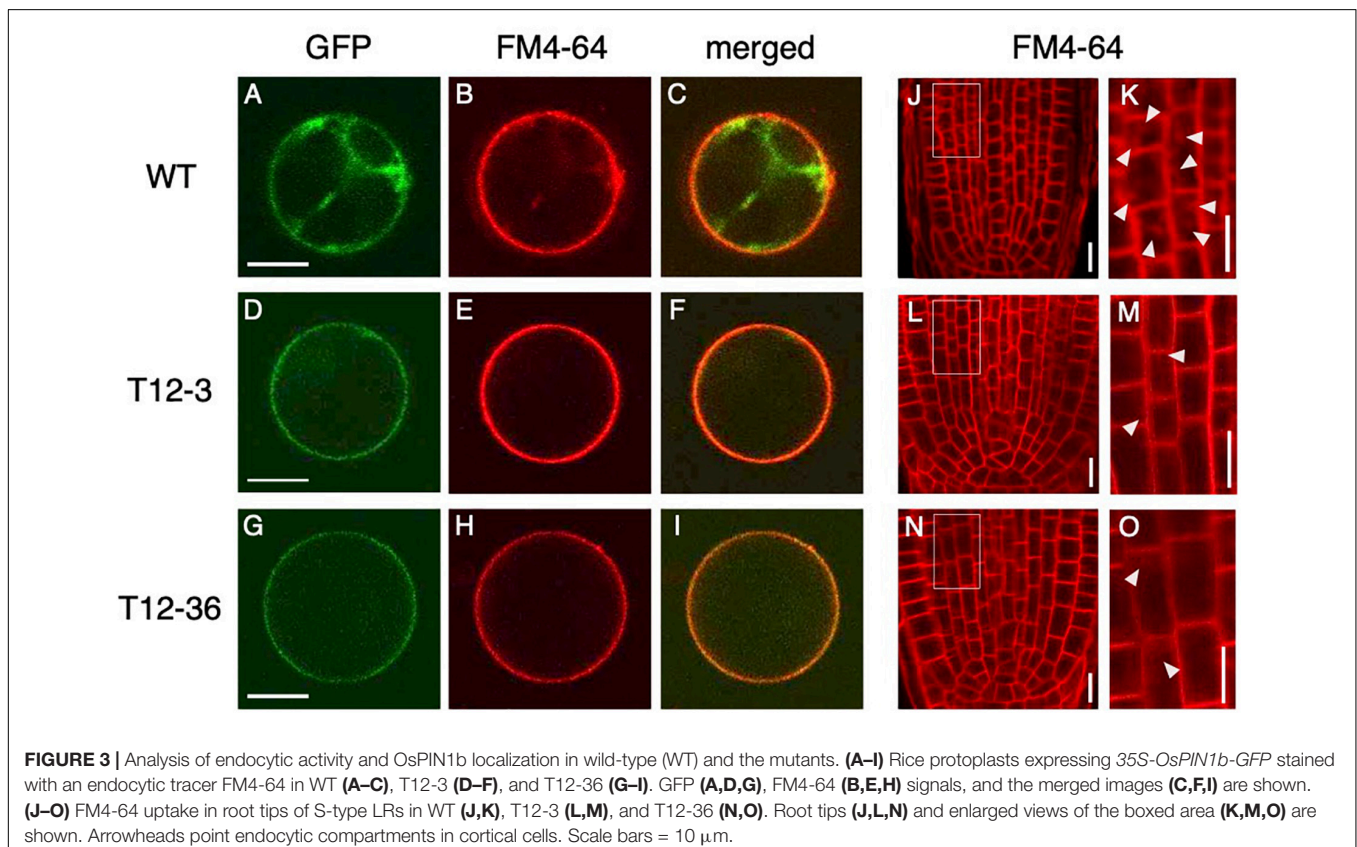
Because dynamin functions in the CME of auxin transporter PIN proteins (Mravec et al., 2011), the mutations in DRPs might affect cellular localization of PIN proteins and hence auxin distribution in LRP. We first analyzed PIN localization and the endocytic activity in rice protoplast of the WT and *drp* mutants. OsPIN1b, which was highly expressed in both S- and

L-type LRP among PIN family genes in the WT (**Supplementary Figure 5**), was fused to GFP and overexpressed in rice protoplast under the 35S promoter. Endocytic activity was monitored with a fluorescent endocytic tracer FM4-64. In WT, OsPIN1b-GFP was detected at plasma membrane and intracellular compartments (**Figure 3A**). FM4-64 was overlapped with the OsPIN1b-GFP signal (**Figures 3B,C**), confirming its localization in the endocytic pathway. In contrast, OsPIN1b-GFP signal was detected at the plasma membrane but absent from intracellular spaces in T12-3 and T12-36 with reduced FM4-64 uptake (**Figures 3D–I**). These observations suggest that OsDRP1C and OsDRP2B function in the endocytosis of OsPIN1b proteins in rice protoplast.

To further analyze if endocytic activity was affected in the roots of *drp* mutants, FM4-64 uptake was analyzed in the roots of WT and *drp* mutants. In WT, FM4-64 was detected at plasma membrane and endosomal compartments in the root tips of S-type LRs (**Figures 3J,K**). In T12-3 and T12-36, FM4-64 was detected at plasma membrane, but its intracellular uptake was reduced (**Figures 3L–O**). Therefore, the mutations in *OsDRP1C* and *OsDRP2B* reduces endocytic activity, affecting PIN protein localization in rice roots.

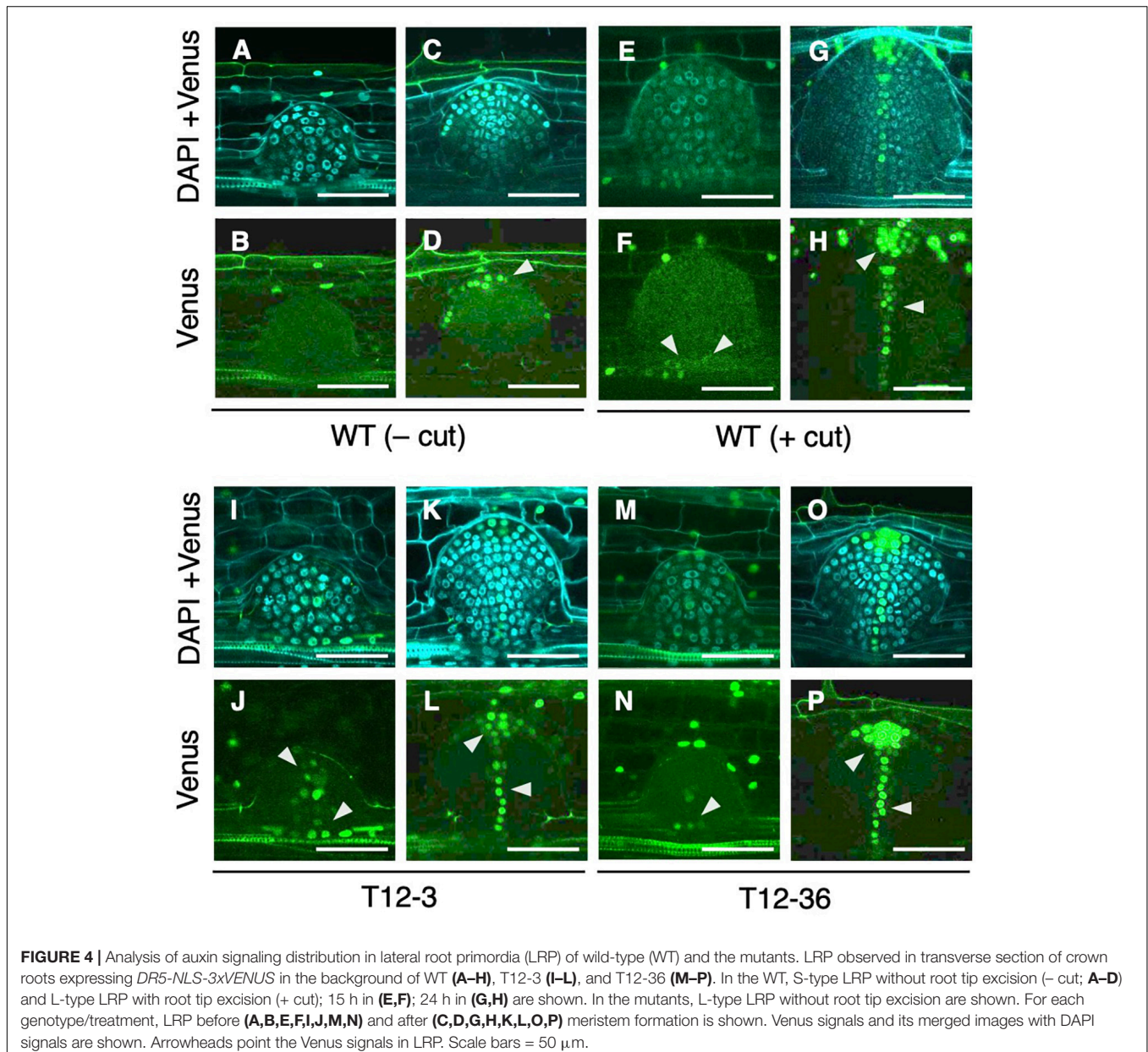
Altered Auxin Distribution in Lateral Root Primordia of *Dynamin-Related Protein* Mutants

Next, we analyzed whether auxin signaling changes in the LRP of the *drp* mutants using a *DR5-NLS-3xVENUS* construct



transformed into T12-3 and T12-36. In the S-type LRP of the WT, Venus signal was detected after meristem formation in root cap cells (Figures 4C,D), but not before meristem formation (Figures 4A,B). Because the WT produced fewer L-type LRs in the control (Figures 1B,D), root tip excision was conducted on CRs to analyze auxin signaling in L-type LRP. In the L-type LRP of the WT, Venus signal was detected in the basal part before the meristem formation, and in the root tip and stele cells in the established meristem (Figures 4E–H). In the mutants, Venus signal was also detected from an early stage in the basal part of LRP (Figures 4I,J,M,N), and in the root tip and stele cells after meristem formation (Figures 4K,L,O,P). Therefore, auxin signaling is upregulated in an early stage of L-type LRP in the WT after root tip excision and in *drp* mutants.

In *Arabidopsis*, PIN1 localization shifts from anticlinal sides toward the tip of LRP during LR formation, forming auxin maxima in the tip (Tanaka et al., 2013). In contrast, the mutations in *BEN1* and *BEN2*, involved in intracellular trafficking of PINs, caused less PIN relocation toward the LRP tip, resulting in broader *DR5* expression and wider LRP than the WT (Tanaka et al., 2013). Therefore, altered auxin distribution could affect LRP diameter. It is noteworthy that the expression of *DRP* family genes did not differ between the S- and L-type LRP (Supplementary Figure 4D). Thus, factor(s) other than DRPs might regulate auxin distribution and LRP size in the WT. It was also suggested that auxin transport and *de novo* biosynthesis is involved in L-type LR formation after root tip excision (Kawai et al., 2022a).



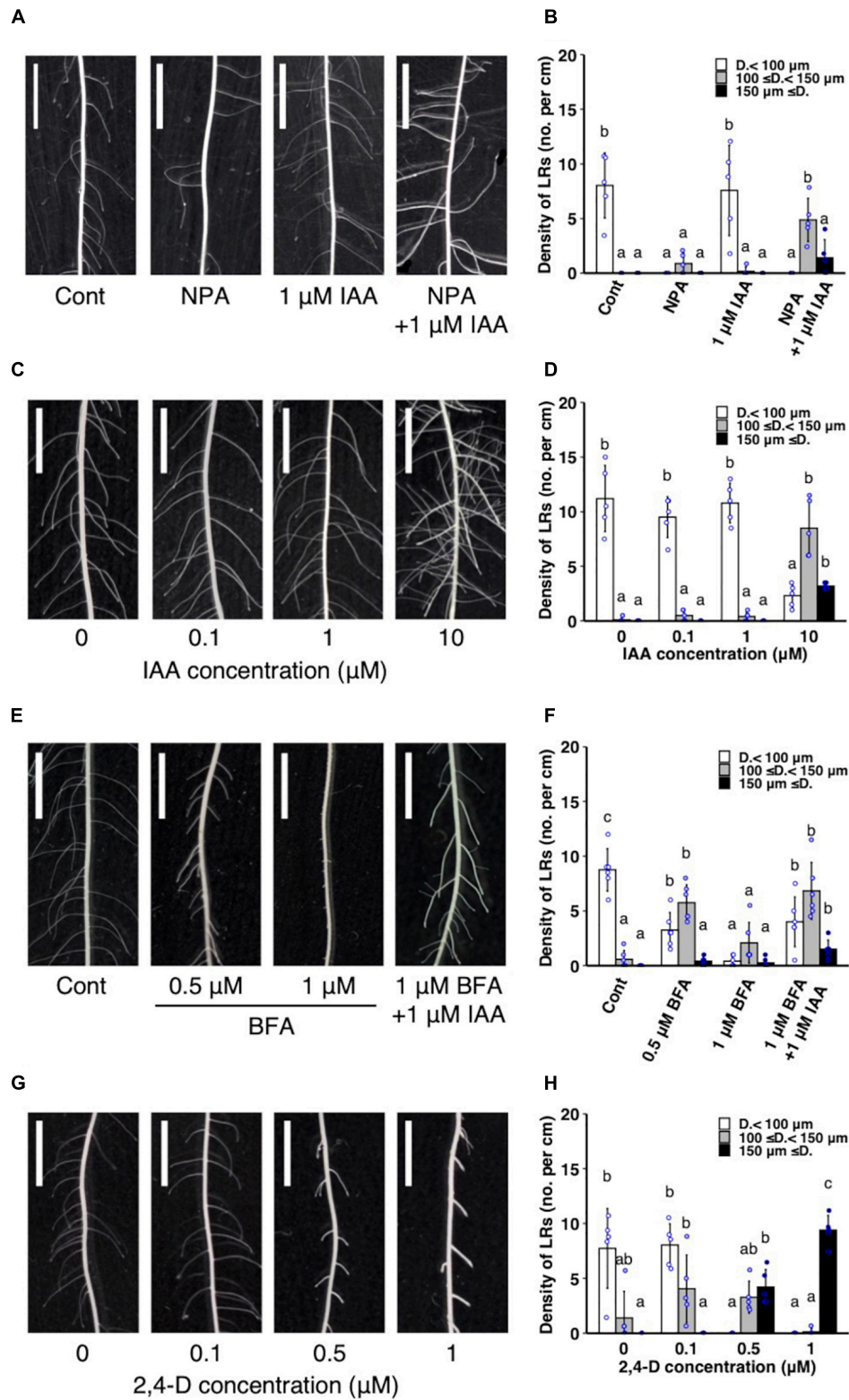
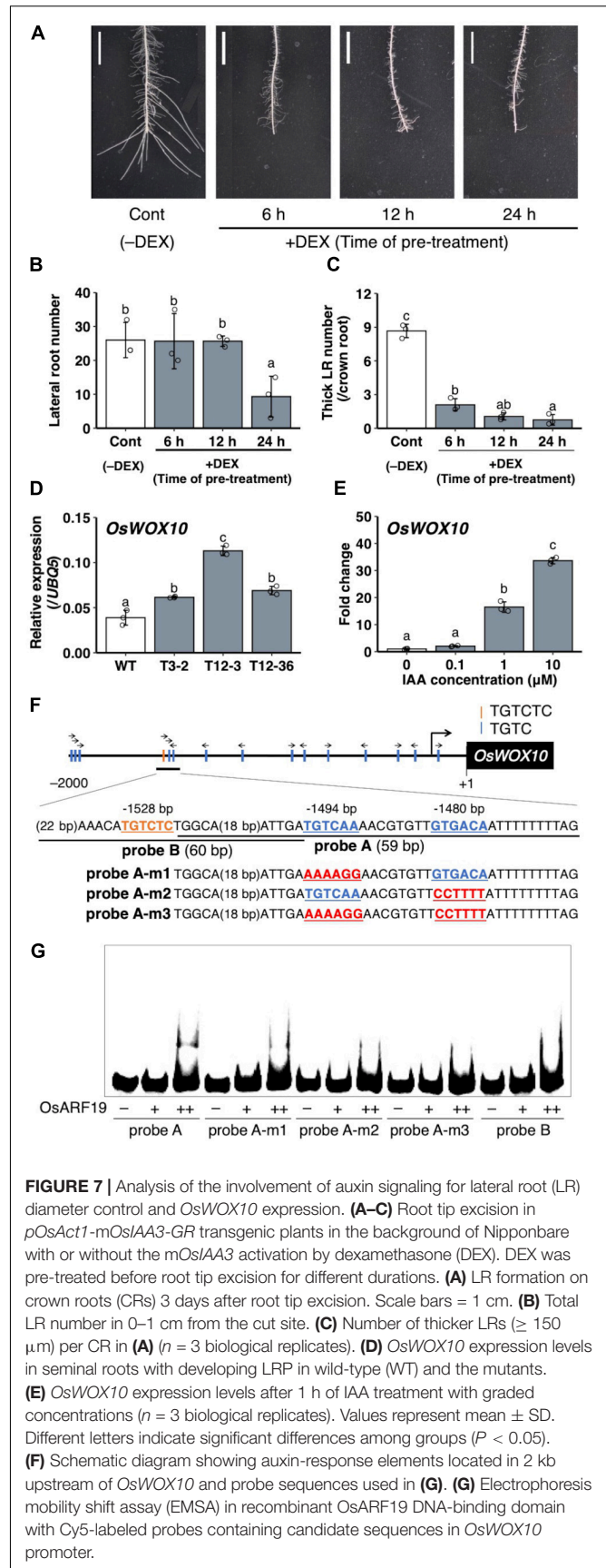
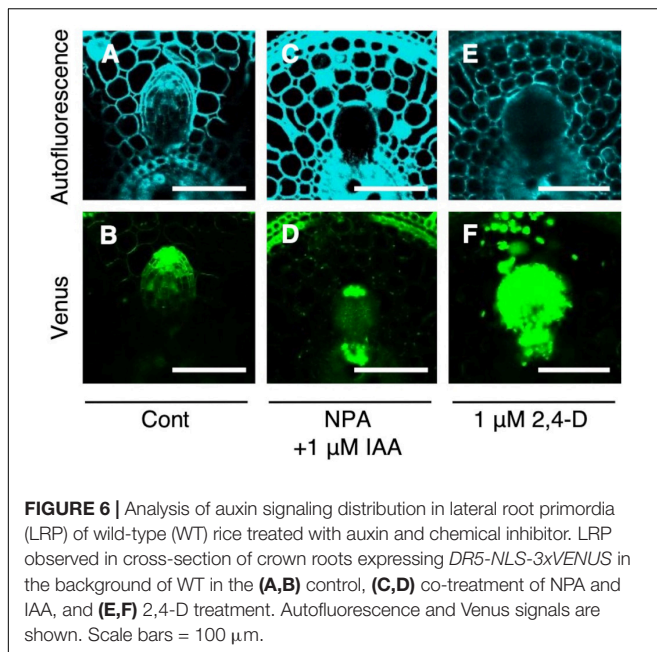


FIGURE 5 | Analysis of the effect of exogenous auxin and chemical inhibitors on lateral root (LR) formation on seminal roots in wild-type rice. **(A,B)** Treatment of IAA and a polar auxin transport inhibitor NPA. **(C,D)** IAA treatment. **(E,F)** Treatment of IAA and a vesicle trafficking inhibitor BFA. **(G,H)** 2,4-D treatment. **(A,C,E,G)** LR formation in control and treated plants. Scale bars = 5 mm. **(B,D,F,H)** Density of LRs in different diameter classes. D., LR diameter. Values represent mean \pm SD ($n = 5$ independent biological replicates). Different letters indicate significant differences among treatments ($P < 0.05$).

Inhibition of Polar Auxin Transport Enhanced L-Type Lateral Roots Formation

The WT plants were treated with auxin transport inhibitors with or without IAA co-treatment to further analyze whether the altered auxin transport is involved in LR diameter control. A single NPA treatment reduced the number of thinner LRs ($<100 \mu\text{m}$) (Figures 5A,B) and did not increase LR diameter (Supplementary Figure 6A). A single IAA treatment induced thicker LRs ($\geq 150 \mu\text{m}$) at a high concentration ($10 \mu\text{M}$) (Figures 5C,D, and Supplementary Figure 6B). In contrast, the co-treatment of a lower concentration of IAA ($1 \mu\text{M}$) and NPA increased LRs with intermediate diameter between S- and L-types ($100\text{--}150 \mu\text{m}$) (Figures 5A,B) and LR diameter (Supplementary Figure 6A). Similarly, a vesicle trafficking inhibitor BFA ($1 \mu\text{M}$) with $1 \mu\text{M}$ IAA increased the thicker LRs ($\geq 150 \mu\text{m}$) (Figures 5E,F). Furthermore, $0.5 \mu\text{M}$ BFA increased the LRs with intermediate diameter ($100\text{--}150 \mu\text{m}$) and LR diameter although $1 \mu\text{M}$ BFA inhibited LR formation (Figures 5E,F and Supplementary Figure 6C). Therefore, the inhibition of polar auxin transport enhanced the effect of exogenous auxin to induce L-type LRs. The 2,4-D is an artificial auxin which moves in plant tissues independent of the polar auxin transport (Sugawara et al., 2015). The 2,4-D treatment induced thicker LRs ($\geq 150 \mu\text{m}$) at a lower concentration ($0.5 \mu\text{M}$) than in IAA treatment (Figures 5G,H and Supplementary Figure 6D), further suggesting that non-directional movement of auxin could increase LR diameter more effectively than polar auxin transport. To analyze if the auxin sensitivity is altered in *drp* mutants, T12-3 and T12-36 were treated with IAA. The lower concentration of IAA ($1 \mu\text{M}$) significantly increased thicker LRs ($\geq 150 \mu\text{m}$) in the mutants but not in WT (Supplementary Figure 6E), suggesting the higher auxin sensitivity in the *drp* mutants than WT.



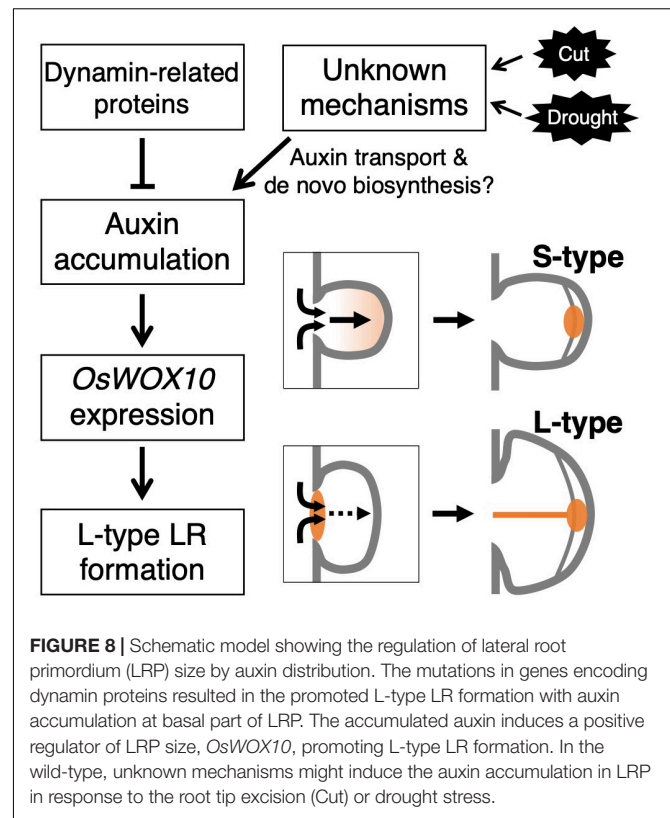
Auxin signaling was observed after the IAA and NPA treatment using *DR5-NLS-3xVENUS* in the WT. After the co-treatment of 1 μM IAA and NPA, Venus signal was detected in the apical and basal part of LRP (Figures 6C,D), but only in apical parts in the control (Figures 6A,B). After the 2,4-D treatment, Venus signal was detected in whole LRP (Figures 6E,F). It is noteworthy that auxin signaling was also upregulated at the basal part of L-type LRP in WT after root tip excision and in *drp* mutants (Figure 4), suggesting that auxin accumulation at the basal part of LRP increases LR diameter.

Repressed L-Type Lateral Roots Formation After Root Tip Excision by Inducible Suppression of Auxin Signaling

To analyze the role of the upregulated auxin signaling in L-type LRP for LR diameter increase, auxin signaling was suppressed by expressing mutagenized *OsIAA3* (*mOsIAA3*), which is not degraded by auxin, using a steroid hormone-inducible system (Nakamura et al., 2006). In this system, the over-expressed *mOsIAA3* by rice *Actin 1* gene promoter is activated by DEX application. In the transgenic Nipponbare plants harboring *pOsAct1-mOsIAA3-GR*, 24 h pre-treatment of DEX decreased LR number after root tip excision (Figures 7A,B). The shorter pre-treatments of DEX (6 and 12 h) did not affect the LR number; however, it decreased the number of thicker LRs that emerged after root tip excision (Figures 7A–C), suggesting the positive role of auxin signaling in LR diameter increase after root tip excision.

Regulation of a Positive Regulator of Lateral Roots Diameter *OsWOX10* Through Auxin Signaling

A *WUSCHEL*-related *homeobox* gene, *OsWOX10*, was identified as a positive regulator of LR diameter, upregulated in L-type LRP in WT after root tip excision (Kawai et al., 2022a). To examine whether *OsWOX10* is involved in thicker LR formation in *drp* mutants, *OsWOX10* expression was measured by qRT-PCR. The *drp* mutants had higher *OsWOX10* expression than the WT in SR segments that include developing LRP (Figure 7D). It is noteworthy that the *OsWOX10* expression level was positively correlated with the maximum LR diameter among the WT and mutants (Figure 1F), suggesting that increased *OsWOX10* expression increases LR diameter in *drp* mutants. *OsWOX10* expression increased after 1 h of the exogenous IAA treatment in WT roots in a dose-dependent manner (Figure 7E). Because 15 AuxREs (TGTCNN) exist in 2 kb upstream region of *OsWOX10* (Figure 7F), the binding of an ARF transcriptional factor, OsARF19, to the AuxREs was tested by performing an EMSA. OsARF19 was selected for its transcriptional activation activity and the positive role in LR formation in rice with the higher expression levels in developing LRP among rice ARF family genes (Yamauchi et al., 2019). The OsARF19 bound to probe A containing two AuxREs facing each other (TGTCAA/GTGACA) but not to probe B including an AuxRE (TGTCTC) (Figure 7G). Mutating one of the AuxREs in probe



A weakened the binding (Figure 7G). Therefore, *OsWOX10* is a potential target of OsARF19.

Notably, auxin signaling was upregulated in LRP, including the basal part in WT after root tip excision and in *drp* mutants (Figure 4), where the *OsWOX10* expression was detected after root tip excision in WT (Kawai et al., 2022a). *OsWOX10* was upregulated by IAA treatment (Figure 7E) and revealed as a potential target of the ARF transcriptional activator in the auxin signaling pathway (Figure 7G). Therefore, auxin signaling upregulation in basal part of LRP induces *OsWOX10* expression, increasing LR diameter. Further analysis of spatial-temporal regulation of auxin distribution in LRP under different environmental conditions is required to reveal the detailed mechanisms of LR diameter regulation.

CONCLUSION

This study revealed the involvement of auxin distribution in LR diameter control (Figure 8). LR diameter increased in *drp* mutants with the upregulated auxin signaling in LRP including the basal part at an early stage. The *drp* mutants had a decreased endocytic activity with reduced PIN protein localization in endosomal compartments. Inhibiting polar auxin transport by NPA and BFA enhanced the effect of exogenous auxin application on LR diameter increase. The co-treatment of IAA and NPA resulted in auxin accumulation in the basal part of LRP. Therefore, it is conceivable that auxin accumulation at the basal part of LRP increases LR diameter. The increased *OsWOX10*

expression was detected by exogenous IAA application and in *drp* mutants. Furthermore, inactivation of auxin signaling by *mOsIAA3-GR* suppressed the L-type LR formation after root tip excision. These data indicate that auxin accumulation in LRP, especially at the basal part, increases LR diameter through *OsWOX10* upregulation.

DATA AVAILABILITY STATEMENT

The original contributions presented in the study are included in the article/**Supplementary Material**, further inquiries can be directed to the corresponding author/s.

AUTHOR CONTRIBUTIONS

TKa and YI conceived, designed the experiments, and wrote the manuscript. TKa, RA, IS, TKo, MS, and HT performed the experiments. TKa, RA, and YI analyzed the data. All authors contributed to the article and approved the submitted version.

REFERENCES

- Abas, L., Kolb, M., Stadlmann, J., Janacek, D. P., Lukic, K., Schwechheimer, C., et al. (2021). Naphthylphthalamic acid associates with and inhibits PIN auxin transporters. *Proc. Natl. Acad. Sci. U.S.A.* 118:e2020857118. doi: 10.1073/pnas.2020857118
- Benková, E., Michniewicz, M., Sauer, M., Teichmann, T., Seifertová, D., Jürgens, G., et al. (2003). Local, efflux-dependent auxin gradients as a common module for plant organ formation. *Cell* 115, 591–602. doi: 10.1016/S0092-8674(03)00924-3
- Colmer, T. D. (2003). Aerenchyma and an inducible barrier to radial oxygen loss facilitate root aeration in upland, paddy and deep-water rice (*Oryza sativa* L.). *Ann. Bot.* 91, 301–309. doi: 10.1093/aob/mcf114
- Dhonukshe, P., Aniento, F., Hwang, I., Robinson, D. G., Mravec, J., Stierhof, Y. D., et al. (2007). Clathrin-mediated constitutive endocytosis of pin auxin efflux carriers in *Arabidopsis*. *Curr. Biol.* 17, 520–527. doi: 10.1016/j.cub.2007.01.052
- Fujimoto, M., Arimura, S. I., Ueda, T., Takahashi, H., Hayashi, Y., Nakano, A., et al. (2010). *Arabidopsis* dynamin-related proteins DRP2B and DRP1A participate together in clathrin-coated vesicle formation during endocytosis. *Proc. Natl. Acad. Sci. U.S.A.* 107, 6094–6099. doi: 10.1073/pnas.0913562107
- Fukaki, H., Tameda, S., Masuda, H., and Tasaka, M. (2002). Lateral root formation is blocked by a gain-of-function mutation in the SOLITARY-ROOT/IAA14 gene of *Arabidopsis*. *Plant J.* 29, 153–168. doi: 10.1046/j.0960-7412.2001.01201.x
- Geldner, N., Anders, N., Wolters, H., Keicher, J., Kornberger, W., Müller, P., et al. (2003). The *Arabidopsis* GNOM ARF-GEF mediates endosomal recycling, auxin transport, and auxin-dependent plant growth. *Cell* 112, 219–230. doi: 10.1016/S0092-8674(03)00003-5
- Gray, W. M., Kepinski, S., Rouse, D., Leyser, O., and Estelle, M. (2001). Auxin regulates SCF^{TR1}-dependent degradation of AUX/IAA proteins. *Nature* 414, 271–276. doi: 10.1038/35104500
- Hiei, Y., Ohta, S., Komari, T., and Kumashiro, T. (1994). Efficient transformation of rice (*Oryza sativa* L.) mediated by *Agrobacterium* and sequence analysis of the boundaries of the T-DNA. *Plant J.* 6, 271–282. doi: 10.1046/j.1365-313X.1994.6020271.x
- Hirano, K., Kotake, T., Kamihara, K., Tsuna, K., Aohara, T., Kaneko, Y., et al. (2010). Rice *BRITTLE CULM 3 (BC3)* encodes a classical dynamin OsDRP2B essential for proper secondary cell wall synthesis. *Planta* 232, 95–108. doi: 10.1007/s00425-010-1145-6
- Inahashi, H., Shelley, I. J., Yamauchi, T., Nishiuchi, S., Takahashi-Nosaka, M., Matsunami, M., et al. (2018). OsPIN2, which encodes a member of the auxin

FUNDING

This work was supported by JSPS KAKENHI (Grant Nos. 18H02174 and 18J21800), the SATREPS Program (JPMJSA1706) of the Japan Science and Technology Agency and Japan International Cooperation Agency, and Nagoya University Research Fund.

ACKNOWLEDGMENTS

We thank Kimiyo Inukai, Eiko Murakami, and Saki Nishiuchi for their valuable technical support, Kotaro Miura for providing the screening lines for rice mutants, the NARO Genebank for providing the rice Full-length cDNA, Mikio Nakazono and Hirokazu Takahashi for their valuable advice, and Kadambot Siddique and Yinglong Chen for revising the manuscript.

SUPPLEMENTARY MATERIAL

The Supplementary Material for this article can be found online at: <https://www.frontiersin.org/articles/10.3389/fpls.2022.834378/full#supplementary-material>

- efflux carrier proteins, is involved in root elongation growth and lateral root formation patterns via the regulation of auxin distribution in rice. *Physiol. Plant.* 164, 216–225. doi: 10.1111/ppl.12707
- Kawai, T., Nosaka-Takahashi, M., Yamauchi, A., and Inukai, Y. (2017). Compensatory growth of lateral roots responding to excision of seminal root tip in rice. *Plant Root* 11, 48–57. doi: 10.3117/plantroot.11.48
- Kawai, T., Chen, Y., Takahashi, H., Inukai, Y., and Siddique, K. H. M. (2022b). Rice genotypes express compensatory root growth with altered root distributions in response to root cutting. *Front. Plant Sci.* 13:830577. doi: 10.3389/fpls.2022.830577
- Kawai, T., Shibata, K., Akahoshi, R., Nishiuchi, S., Takahashi, H., Nakazono, M., et al. (2022a). WUSCHEL-related homeobox family genes in rice control lateral root primordia size. *Proc. Natl. Acad. Sci. U.S.A.* 119:e2101846119. doi: 10.1073/pnas.2101846119
- Kawata, S., and Shibayama, B. (1965). On the lateral root primordia formation in the crown roots of rice plant. *Proc. Crop Sci. Soc. Japan* 33, 423–431. doi: 10.1626/jcs.33.423
- Kitakura, S., Vanneste, S., Robert, S., Löfke, C., Teichmann, T., Tanaka, H., et al. (2011). Clathrin mediates endocytosis and polar distribution of PIN auxin transporters in *Arabidopsis*. *Plant Cell* 23, 1920–1931. doi: 10.1105/tpc.111.083030
- Kitomi, Y., Inahashi, H., Takehisa, H., Sato, Y., and Inukai, Y. (2012). OsIAA13-mediated auxin signaling is involved in lateral root initiation in rice. *Plant Sci.* 190, 116–122. doi: 10.1016/j.plantsci.2012.04.005
- Kitomi, Y., Ogawa, A., Kitano, H., and Inukai, Y. (2008). CRL4 regulates crown root formation through auxin transport in rice. *Plant Root* 2, 19–28. doi: 10.3117/plantroot.2.19
- Kleine-Vehn, J., Dhonukshe, P., Sauer, M., Brewer, P. B., Wiśniewska, J., Paciorek, T., et al. (2008). ARF GEF-dependent transcytosis and polar delivery of PIN auxin carriers in *Arabidopsis*. *Curr. Biol.* 18, 526–531. doi: 10.1016/j.cub.2008.03.021
- Kleine-Vehn, J., Wabnik, K., Martinière, A., Łągowski, Ł., Willig, K., Naramoto, S., et al. (2011). Recycling, clustering, and endocytosis jointly maintain PIN auxin carrier polarity at the plasma membrane. *Mol. Syst. Biol.* 7:540. doi: 10.1038/msb.2011.72
- Kono, Y., Igeta, M., and Yamada, N. (1972). Studies on the developmental physiology of the lateral roots in rice seminal roots. *Proc. Crop Sci. Soc. Japan* 41, 192–204. doi: 10.1626/jcs.41.192

- Li, Y., Zhu, J., Wu, L., Shao, Y., Wu, Y., and Mao, C. (2019). Functional divergence of PIN1 paralogous genes in rice. *Plant Cell Physiol.* 60, 2720–2732. doi: 10.1093/pcp/pcz159
- Liu, S., Wang, J., Wang, L., Wang, X., Xue, Y., Wu, P., et al. (2009). Adventitious root formation in rice requires OsGNOM1 and is mediated by the OsPINs family. *Cell Res.* 19, 1110–1119. doi: 10.1038/cr.2009.70
- Love, M. I., Huber, W., and Anders, S. (2014). Moderated estimation of fold change and dispersion for RNA-seq data with DESeq2. *Genome Biol.* 15:550. doi: 10.1186/s13059-014-0550-8
- Lucob-Agustin, N., Kawai, T., Kano-Nakata, M., Suralta, R. R., Niones, J. M., Hasegawa, T., et al. (2021). Morpho-physiological and molecular mechanisms of phenotypic root plasticity for rice adaptation to water stress conditions. *Breed. Sci.* 71, 20–29. doi: 10.1270/jsbbs.20106
- Lucob-Agustin, N., Kawai, T., Takahashi-Nosaka, M., Kano-Nakata, M., Wainaina, C. M., Hasegawa, T., et al. (2020). WEG1, which encodes a cell wall hydroxyproline-rich glycoprotein, is essential for parental root elongation controlling lateral root formation in rice. *Physiol. Plant.* 169, 214–227. doi: 10.1111/ppl.13063
- Luschign, C., and Vert, G. (2014). The dynamics of plant plasma membrane proteins: PINs and beyond. *Development* 141, 2924–2938. doi: 10.1242/dev.103424
- Mravec, J., Petrášek, J., Li, N., Boeren, S., Karlova, R., Kitakura, S., et al. (2011). Cell plate restricted association of DRP1A and PIN proteins is required for cell polarity establishment in *Arabidopsis*. *Curr. Biol.* 21, 1055–1060. doi: 10.1016/j.cub.2011.05.018
- Nakagawa, T., Suzuki, T., Murata, S., Nakamura, S., Hino, T., Maeo, K., et al. (2007). Improved gateway binary vectors: high-performance vectors for creation of fusion constructs in transgenic analysis of plants. *Biosci. Biotechnol. Biochem.* 71, 2095–2100. doi: 10.1271/bbb.70216
- Nakamura, A., Umemura, I., Gomi, K., Hasegawa, Y., Kitano, H., Sazuka, T., et al. (2006). Production and characterization of auxin-insensitive rice by overexpression of a mutagenized rice IAA protein. *Plant J.* 46, 297–306. doi: 10.1111/j.1365-313X.2006.02693.x
- Ozawa, K. (2009). Establishment of a high efficiency *Agrobacterium*-mediated transformation system of rice (*Oryza sativa* L.). *Plant Sci.* 176, 522–527. doi: 10.1016/j.plantsci.2009.01.013
- R Core Team (2020). *R: A language and environment for statistical computing*. (Vienna: R Foundation for Statistical Computing).
- Ramachandran, R., Surka, M., Chappie, J. S., Fowler, D. M., Foss, T. R., Song, B. D., et al. (2007). The dynamin middle domain is critical for tetramerization and higher-order self-assembly. *EMBO J.* 26, 559–566. doi: 10.1038/sj.emboj.7601491
- Ramos, J. A., Zenser, N., Leyser, O., Callis, J. (2001). Rapid degradation of auxin/indoleacetic acid proteins requires conserved amino acids of domain II and is proteasome dependent. *Plant Cell* 13, 2349–2360. doi: 10.1105/tpc.13.10.2349
- Sasaki, O., Yamazaki, K., and Kawata, S. (1984). The development of lateral root primordia in rice plants. *Jpn. J. Crop Sci.* 53, 169–175. doi: 10.1626/jcs.53.169
- Sato, H., and Omura, T. (1979). Induction of mutation by the treatment of fertilized egg cell with N-methyl-N-nitrosourea in rice. *J. Fac. Agric. Kyushu Univ.* 24, 165–174. doi: 10.5109/23706
- Sato, Y., Namiki, N., Takehisa, H., Kamatsuki, K., Minami, H., Ikawa, H., et al. (2013a). RiceFRIEND: a platform for retrieving coexpressed gene networks in rice. *Nucleic Acids Res.* 41, 1214–1221. doi: 10.1093/nar/gks1122
- Sato, Y., Takehisa, H., Kamatsuki, K., Minami, H., Namiki, N., Ikawa, H., et al. (2013b). RiceXPro version 3.0: expanding the informatics resource for rice transcriptome. *Nucleic Acids Res.* 41, 1206–1213. doi: 10.1093/nar/gks1125
- Sato, M., Akashi, H., Sakamoto, Y., Matsunaga, S., and Tsuji, H. (2022). Whole-Å tissue three-dimensional imaging of rice at single-Å cell resolution. *Int. J. Mol. Sci.* 23:40. doi: 10.3390/ijms23010040
- Sakamoto, Y., Ishimoto, A., Sakai, Y., Sato, M., Nishihama, R., Abe, K., et al. (2022). Improved clearing method contributes to deep imaging of plant organs. *Commun. Biol.* 5:12. doi: 10.1038/s42003-021-02955-9
- Schmid, S. L., and Frolov, V. A. (2011). Dynamin: functional design of a membrane fission catalyst. *Annu. Rev. Cell Dev. Biol.* 27, 79–105. doi: 10.1146/annurev-cellbio-100109-104016
- Sreevidya, V. S., Hernandez-Oane, R. J., Gyaneshwar, P., Lara-Flores, M., Ladha, J. K., and Reddy, P. M. (2010). Changes in auxin distribution patterns during lateral root development in rice. *Plant Sci.* 178, 531–538. doi: 10.1016/j.plantsci.2010.03.004
- Steinmann, T., Geldner, N., Grebe, M., Mangold, S., Jackson, C. L., Paris, S., et al. (1999). Coordinated polar localization of auxin efflux carrier PIN1 by GNOM ARF GEF. *Science* 286, 316–318. doi: 10.1126/science.286.5438.316
- Sugawara, S., Mashiguchi, K., Tanaka, K., Hishiyama, S., Sakai, T., Hanada, K., et al. (2015). Distinct characteristics of indole-3-acetic acid and phenylacetic acid, two common auxins in plants. *Plant Cell Physiol.* 56, 1641–1654. doi: 10.1093/pcp/pcv088
- Sun, H., Xu, F., Guo, X., Wu, D., Zhang, X., Lou, M., et al. (2019). A strigolactone signal inhibits secondary lateral root development in rice. *Front. Plant Sci.* 10:1527. doi: 10.3389/fpls.2019.01527
- Suralta, R. R., Kano-Nakata, M., Niones, J. M., Inukai, Y., Kameoka, E., Tran, T. T., et al. (2018). Root plasticity for maintenance of productivity under abiotic stressed soil environments in rice: progress and prospects. *Field Crops Res.* 220, 57–66. doi: 10.1016/j.fcr.2016.06.023
- Tan, X., Calderon-Villalobos, L. I. A., Sharon, M., Zheng, C., Robinson, C. V., Estelle, M., et al. (2007). Mechanism of auxin perception by the TIR1 ubiquitin ligase. *Nature* 446, 640–645. doi: 10.1038/nature05731
- Tanaka, H., Kitakura, S., Rakusová, H., Uemura, T., Feraru, M. I., De Rycke, R., et al. (2013). Cell polarity and patterning by PIN trafficking through early endosomal compartments in *Arabidopsis thaliana*. *PLoS Genet.* 9:e1003540. doi: 10.1371/journal.pgen.1003540
- Watanabe, Y., Kabuki, T., Kakehashi, T., Kano-Nakata, M., Mitsuya, S., and Yamauchi, A. (2020). Morphological and histological differences among three types of component roots and their differential contribution to water uptake in the rice root system. *Plant Prod. Sci.* 23, 191–201. doi: 10.1080/1343943X.2020.1730701
- Xiong, G., Li, R., Qian, Q., Song, X., Liu, X., Yu, Y., et al. (2010). The rice dynamin-related protein DRP2B mediates membrane trafficking, and thereby plays a critical role in secondary cell wall cellulose biosynthesis. *Plant J.* 64, 56–70. doi: 10.1111/j.1365-313X.2010.04308.x
- Xu, M., Zhu, L., Shou, H., and Wu, P. (2005). A PIN1 family gene, OsPIN1, involved in auxin-dependent adventitious root emergence and tillering in rice. *Plant Cell Physiol.* 46, 1674–1681. doi: 10.1093/pcp/pci183
- Yamauchi, A., Kono, Y., and Tatsumi, J. (1987). Quantitative analysis on root system structures of upland rice and maize. *Jpn. J. Crop Sci.* 56, 608–617. doi: 10.1626/jcs.56.608
- Yamauchi, T., Tanaka, A., Inahashi, H., Nishizawa, N. K., Tsutsumi, N., Inukai, Y., et al. (2019). Fine control of aerenchyma and lateral root development through AUX/IAA- and ARF-dependent auxin signaling. *Proc. Natl. Acad. Sci. U.S.A.* 116, 20770–20775. doi: 10.1073/pnas.1907181116
- Yu, P., Gutjahr, C., Li, C., and Hochholdinger, F. (2016). Genetic control of lateral root formation in cereals. *Trends Plant Sci.* 21, 951–961. doi: 10.1016/j.tplants.2016.07.011
- Zhang, Y., Su, J., Duan, S., Ao, Y., Dai, J., Liu, J., et al. (2011). A highly efficient rice green tissue protoplast system for transient gene expression and studying light/chloroplast-related processes. *Plant Methods* 7:30. doi: 10.1186/1746-4811-7-30
- Zhao, H., Ma, T., Wang, X., Deng, Y., Ma, H., Zhang, R., et al. (2015). OsAUX1 controls lateral root initiation in rice (*Oryza sativa* L.). *Plant Cell Environ.* 38, 2208–2222. doi: 10.1111/pce.12467

Conflict of Interest: The authors declare that the research was conducted in the absence of any commercial or financial relationships that could be construed as a potential conflict of interest.

Publisher's Note: All claims expressed in this article are solely those of the authors and do not necessarily represent those of their affiliated organizations, or those of the publisher, the editors and the reviewers. Any product that may be evaluated in this article, or claim that may be made by its manufacturer, is not guaranteed or endorsed by the publisher.

Copyright © 2022 Kawai, Akahoshi, Shelley, Kojima, Sato, Tsuji and Inukai. This is an open-access article distributed under the terms of the Creative Commons Attribution License (CC BY). The use, distribution or reproduction in other forums is permitted, provided the original author(s) and the copyright owner(s) are credited and that the original publication in this journal is cited, in accordance with accepted academic practice. No use, distribution or reproduction is permitted which does not comply with these terms.